Distinguishing of Oligosaccharide Linkage Isomers by Nanoparticle-assisted Fragmentation in MALDI-TOF MS

Primadona Indah[1]*, Dedi[2], Wang Yi-Sheng[3] and Chen Yu-Ju[4]
1. Research Unit for Clean Technology-Indonesian Institute of Sciences, Bandung, INDONESIA
2. Research Center for Electronica & Telecommunication-Indonesian Institute of Sciences, Bandung, INDONESIA
3. Genomic Research Center-Academia Sinica, Taipei, TAIWAN
4. Institute of Chemistry-Academia Sinica, Taipei, TAIWAN
*indah_primadona@yahoo.com

Abstract
Protein glycosylation plays a critical role in the regulation of numerous biological processes. Aberrations on the glycosylation may lead to alterations in protein function and thus associated with many types of diseases. The structural elucidation of glycan/carbohydrates is challenging due to the complexity and diversity of carbohydrate structure. Recently, nanoparticle-assisted MALDI-TOF MS has been developed for the identification of various analytes including carbohydrate.

Herein, we report a straight-forward approach for simultaneous identification and differentiation of two oligosaccharide linkage isomers (isomaltohexaose and laminarihexaose) by 2,5-dihydoxybenzoic acid functionalized HgTe nanoparticles (HgTe@DHB NPs)-assisted MALDI-TOF MS. This method produced more abundant glycosidic cleavages (Y/B-type ions) and cross-ring fragmentation ions (A/X-type ions) for sequence and linkage analysis respectively as well as provided better signal fragment ion intensity and background-free-spectra compared to conventional matrix.

Keywords: Mass spectrometry, MALDI-TOF MS, Nanoparticle, Fragmentation, Carbohydrate

Introduction

Carbohydrate structural changes are closely related to numerous diseases such as cancer, inflammation and cardiovascular disease[1,2]. Accordingly, comprehensive structural analyses become an interesting field to be studied recently. However, the structure characterization of carbohydrate is more challenging than other classes of biomolecules. Unlike proteins, which possess predominantly linear structure, glycan may exhibit incredibly complicated structures with a large number of monosaccharide units having diversity in composition, sequence, branching, linkage and anomericity.

Furthermore, carbohydrates often exist as various isomeric forms with difference in glycosidic linkage type and position. Traditionally, carbohydrate isomerism are studied by nuclear magnetic resonance (NMR)[3] and tandem mass spectrometry (MS/MS)[4]. However, due to the robustness, mass spectrometry techniques were widely used for this study. In typical MS/MS spectra, glycosidic bond and cross-ring cleavage fragment ions are observed. Glycosidic cleavage occurs between monosaccharide units to generate different Y-, B-, Z- and C-type ions. However, cross-ring cleavages involve the dissociation of two carbon-carbon (C-C) bonds on the same sugar residue to yield A- and X-type ions (fragment ion assignments follow Domon and Costello nomenclature)[5]. The generated unique fragment ions either glycosidic or cross-ring fragments by MS/MS approach were used to distinguish those isomers[6].

Recently, the nanoparticles have been explored as a detection element in various applications including optical spectroscopy[7,8] and matrix-assisted laser desorption/ionization mass spectrometry (MALDI-MS)[9,10]. In MALDI-MS, nanomaterials serve as laser energy-absorber which converts the laser power into thermal energy, then dissipates them to the analyte leading to its desorption and ionization, similar to the role of commonly organic MALDI matrix [2,5-dihydoxybenzoic acid (DHB), α-cyano-4-hydroxycinnamic acid (CHCA), Sinapinic acid (SA) etc.][11] However, in contrast to organic molecule, nanomaterials can efficiently convert the electromagnetic energy of a laser pulse into heat with a significant increase in the local temperature leading to more efficient energy transfer from their surfaces to the analytes[12].

Furthermore, photoelectrons have been implicated in the decomposition of oligosaccharide molecules by the use of magnetic and HgTe NPs as desorption element[13,14]. Without employing the MS/MS technique, HgTe@DHB NPs promoted the dissociation process of complex carbohydrates providing the complete information of their composition, sequence, branching and linkage[14]. Due to their high potential, in this work, the efficacy of HgTe@DHB NPs in MALDI-TOF MS was further tested for differentiating the two linkage isomeric oligosaccharide molecules (isomaltohexaose and laminarihexaose).

Material and Methods

All chemicals and reagents were used as received without further purification. Citric acid monohydrate ($\geq$ 99%), HCl ($\geq$37%), NaOH ($\geq$ 98%), NH4OH (25%), sodium borohydride (NaBH4), mercaptopropionic acid (MPA), cyclohexane, TritonX-100, BaSO4 and iso-propyl alcohol were obtained from Sigma-Aldrich, 2,5-dihydroxybenzoic acid (DHB) from Sigma and Ethanol (Absolute) from J.T. Baker. Tetraethyl orthosilicate (TEOS, $\geq$ 98%), Mercury

chloride (HgCl$_2$), tellurium powder, acetone and butanol were purchased from Acros Organics. 1-hexanol was obtained from Merck.

Analysis of Carbohydrate: Synthesized HgTe@DHB NPs[14] (1 mg) was suspended in 0.1 mL of DI water to give a 10.000 µg mL^{-1} stock solution. Afterwards, it was diluted with DI water to give several concentrations for subsequent MALDI-TOF MS acquisition. In the same manner, the commercial DHB matrix (1 mg) was dissolved in 0.1 mL of DI water to yield a 10.000 µg mL^{-1} working matrix solution. All carbohydrate compounds were dissolved in DI water to yield a 1000 µg mL^{-1} working solution.

For carbohydrate molecule analysis, 1.0 µL of 1000 µg mL^{-1} sample solution was mixed with 1.0 µL of HgTe@DHB working solution and 1.0 µL of the resulting mixture was spotted onto the stainless steel sample plate, air-dried and analyzed in the MALDI-TOF/TOF MS instrument (ABI/SCIEX 4800, Houston, USA; Nd:YAG laser at 355 nm).

Infrared Emission Measurement: The thermal energy of matrix changes the surface temperature and emits IR radiation[15]. Thus, in order to monitor the surface temperature, the IR emission was measured. Infrared emission was detected using a laboratory-built instrument[14]. Briefly, samples were prepared by the conventional dried-droplet method to be compatible with the condition of the mass spectrometric analysis and put into the vacuum chamber. The samples were irradiated by a third harmonic Nd: YAG laser with the fluence approximately 355 J/m^2. The data were obtained from the average of about 200 laser shots.

Threshold Energy of Photoelectron Measurement: A laboratory-built time-of-flight (TOF) mass spectrometer was constructed for measuring the photoelectron of NPs as reported before[14]. NPs were deposited on a stainless-steel sample plate. Laser-induced photoelectrons were extracted through an accelerating potential of 5 kV into the TOF analyzer (225 mm) and detected by a multichannel plate detector. To determine the threshold energy required for generating the photoelectron, the signal-to-noise (S/N) ratio of 3 was utilized.

Results and Discussion
Comparative Evaluation of Fragmentation Efficiency of HgTe@DHB NPs with DHB matrix: In this study, the performance of HgTe@DHB NPs and conventional organic MALDI matrix (DHB) in fragment ion production for carbohydrate characterization in MALDI MS was evaluated. The linear carbohydrate isomaltohexaose which consists of six glucose units was used as a model compound (figure 3a). The mixed sample solution with either HgTe@DHB NPs or DHB was irradiated with the same laser power to acquire the MALDI MS spectra. As shown in figure 1a, DHB matrix generated very few fragments, only two fragment ions can

be observed with low ion intensity. Moreover, the abundant and high intensity matrix-derived ion peaks observed in DHB MS spectra (figure 1a) would interfere and suppress the carbohydrate fragment peaks.

On the contrary, HgTe@DHB NPs produced much cleaner spectra (very few matrix-derived ion peaks) with abundant and high fragment ion intensity both glycosidic and cross-ring cleavage fragments (figure 1b). This result implies that the HgTe@DHB NPs supplied higher energy to induce better ionization and more extensive fragmentation of the analyte than DHB matrix.

Differentiation of Linkage Isomeric Carbohydrate Isomaltohexaose and Laminarihexaose: According to the above and previous results[14], we evaluated further the potency of this NP to discriminate the two-linkage isomeric linear oligosaccharides: isomaltohexaose (figure 3a) and laminarihexaose (figure 3b). Those two molecules are composed of six glucose molecules but differ in the linkage type. Six glucose in isomaltohexaose are connected by α1,6-linkage, while laminarihexaose is α1-3-linked structure. The MS spectrum of isomaltohexaose and laminarihexaose is depicted in figure 2a and 2b respectively while the fragment ion assignments were presented in figure 3 and table 1. As shown in the figure 2, those two isomers can be easily differentiated by the presence of unique cross-ring cleavage A_n ions.

The characteristic $^{0,2}A$ fragment ion series ($^{0,2}A_6$ (*m/z* 953.1), $^{0,2}A_5$ (*m/z* 791.1), $^{0,2}A_4$ (*m/z* 629.1), $^{0,2}A_3$ (*m/z* 467.1) and $^{0,2}A_2$ (*m/z* 305.1)) only appear in the isomaltohexaose but not in the laminarihexaose MS spectrum. It might be due to the formation of $^{0,2}A$ fragment ions in α(1-3) linkage compound requiring higher energy. The distinction of those two isomers was based not mainly on the differences in the ions yielded, but also on the intensities of the ions. Accordingly, the intensity of glycosidic cleavage fragment ions: Y-ions (i.e., *m/z* 851.1, 689.1, 527.1, 365.1) and B-ions (i.e. *m/z* 833.1, 671.1, 509.1, 347.1) of laminarihexaose are 3-20 times higher than isomaltohexaose. As a result, HgTe@DHB NPs-assisted LDI-TOF MS approach indeed could be applied to discriminate the linkage isomeric oligosaccharides.

Comparison of Physical Properties of HgTe@DHB NPs and DHB matrix: As reported previously, the heat and photoelectron released by matrix influenced the fragmentation efficiency in MALDI MS[14]. The high thermal energy and the abundance of photoelectron in the ion source induced the dissociation of glycosidic and intra-ring C-C bonds of carbohydrate. Accordingly, in order to support the proposed "surface-enhanced carbohydrate decomposition" mechanism[14], we evaluated those two physical properties toward HgTe@DHB NPs and DHB and correlate them with the fragmentation degree (figure 1). HgTe@DHB NPs generated the IR emission 4-folds higher than DHB (figure

4a). It means that with the same laser power the surface temperature of HgTe@DHB NPs is higher than DHB.

However, the opposite occurs in the measurement of threshold energy for generating the photoelectrons. To get the same signal intensity of photoelectron, DHB is two times easier than HgTe@DHB NPs (figure 4b). It indicates that DHB matrix released more abundant electron than HgTe@DHB NPs in the same laser fluence.

The trend results are generally consistent with the fragmentation degree (figure 1) and the proposed mechanism[14]. Both photoelectron and heat triggered the dissociation process. However, besides inducing the fragmentation, heat also facilitates the desorption and ionization process. That is the reason why the number and the intensity of fragment ions generated by HgTe@DHB NPs (figure 1b) are higher than that of DHB.
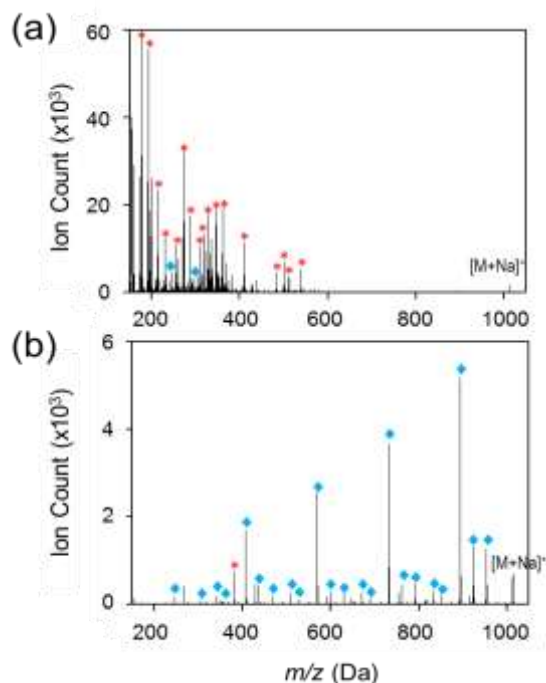

Figure 1: Comparison of MALDI-TOF MS spectra of Isomaltohexaose obtained by different MALDI matrix (a) DHB and (b) HgTe@DHB NPs. The [M+Na]+, (*) and (♦) denote sodium-adducted precursor ions, matrix-derived ion peaks and fragment ion peaks respectively.
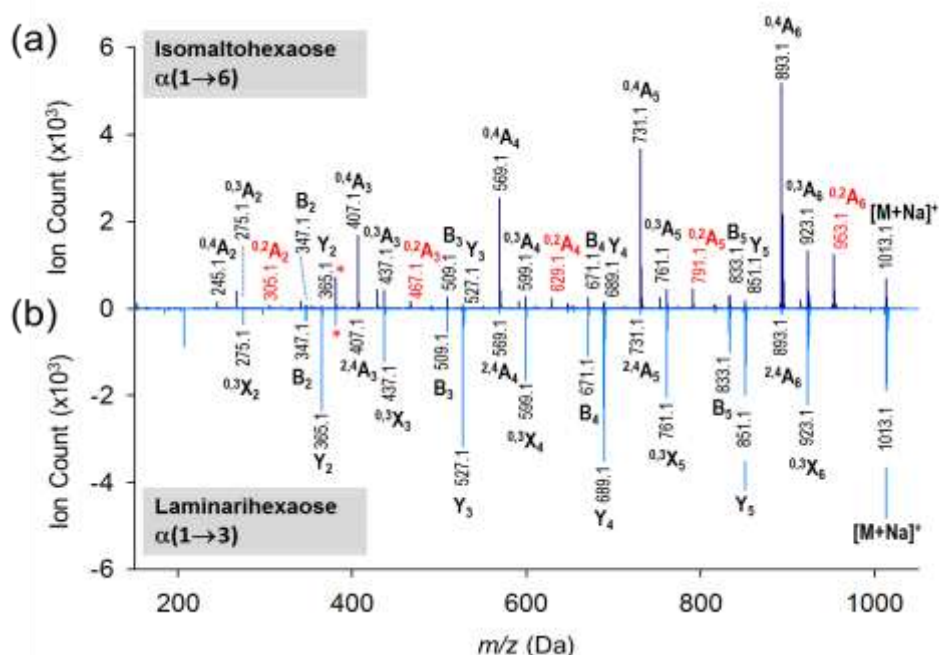

Figure 2: Structural linkage isomer differentiation of Isomaltohexaose (a) and Laminarihexaose (b). [M+Na]+, (*) and red annotation denote sodium adducted precursor ion, NP-derived ion peaks, specific fragments for differentiating those two isomers respectively

*Research Journal of Chemistry and Environment*_____Vol. **22(Special Issue II)** August **(2018)**
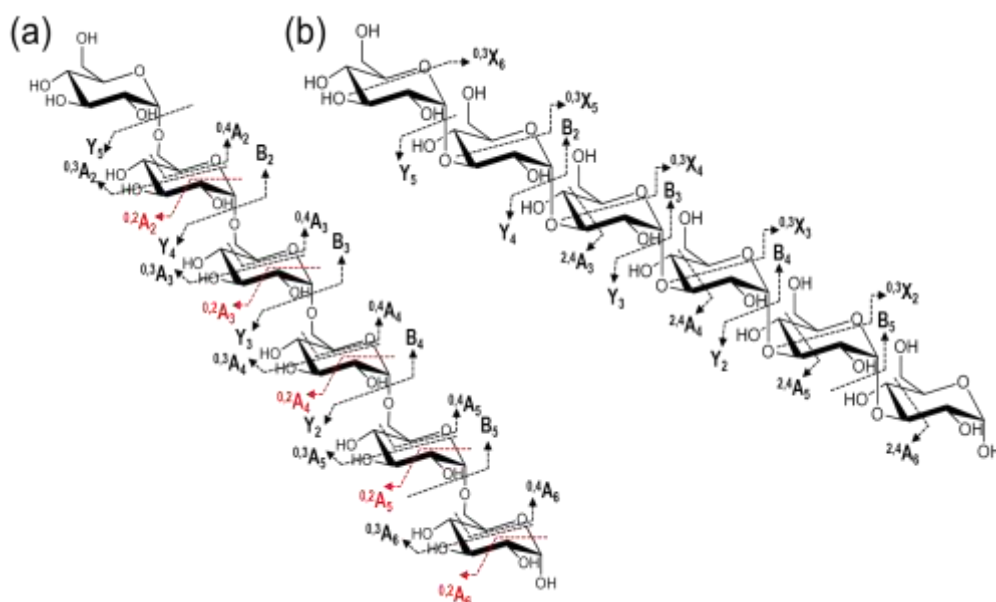
Res. J. Chem. Environ.

Figure 3: Fragmentation patterns including their fragment ion assignments of Isomaltohexaose (a) and Laminarihexaose (b). Red annotation for differentiating those two isomers.

Table 1
Diagnostic fragment ions delineating structural features of Isomaltohexaose and Laminarihexaose HgTe@DHB NP-assisted LDI MS

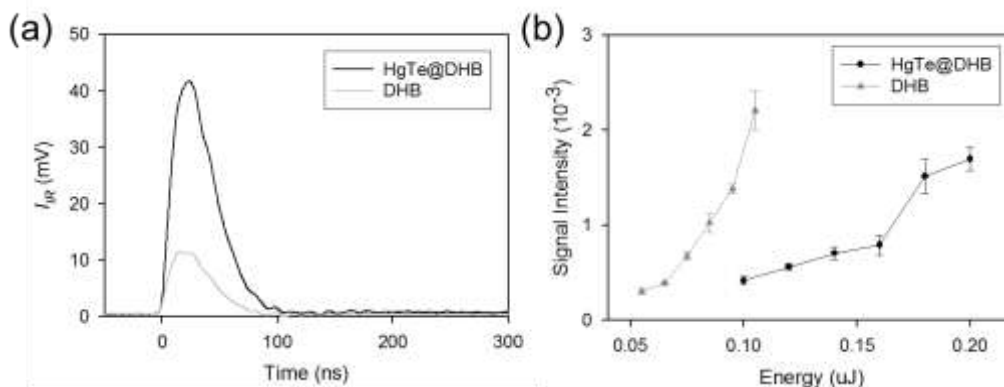| Isomaltohexaose			Laminarihexaose		
Structural Feature	Ion	*m/z* (Da)	Structural Feature	Ion	*m/z* (Da)
Sequence	Y_5	851.1221	Sequence	Y_5	851.1625
	Y_4	689.1088		Y_4	689.1500
	Y_3	527.1067		Y_3	527.1257
	Y_2	365.0856		Y_2	365.0939
	B_5	833.1155		B_5	833.1545
	B_4	671.0999		B_4	671.1414
	B_3	509.0968		B_3	509.1219
	B_2	347.0819		B_2	347.0906
Linkage	$^{0,3}A_6$	923.1242	Linkage	$^{0,3}X_6$	923.1656
	$^{0,3}A_5$	761.1083		$^{0,3}X_5$	761.1467
	$^{0,3}A_4$	599.1019		$^{0,3}X_4$	599.1254
	$^{0,3}A_3$	437.1316		$^{0,3}X_3$	437.1042
	$^{0,3}A_2$	275.0577		$^{0,3}X_2$	275.0618
	$^{0,4}A_6$	893.1208		$^{2,4}A_6$	893.1520
	$^{0,4}A_5$	731.1054		$^{2,4}A_5$	731.1465
	$^{0,4}A_4$	569.0977		$^{2,4}A_4$	569.1324
	$^{0,4}A_3$	407.0869		$^{2,4}A_3$	407.1031
	$^{0,4}A_2$	245.0435		-	-
	$^{0,2}A_6$	953.1281		-	-
	$^{0,2}A_5$	791.1077		-	-
	$^{0,2}A_4$	629.1056		-	-
	$^{0,2}A_3$	467.0987		-	-
	$^{0,2}A_2$	305.0678		-	-

Figure 4: (a) The IR emission signal intensity and threshold photoelectron signal intensity as a function of laser energy of DHB (Grey line) and (b) HgTe@DHB NPs (Black line) matrix.

Conclusion

In summary, the differentiation of two linkage isomeric oligosaccharides has been demonstrated. By utilizing the unique ^{0,2}A-type cross-ring fragment ions and the difference ion intensity of Y and B fragments, the isomeric 1,6-linked and 1,3-linked oligosaccharides can be unambiguously distinguished.

Acknowledgement

References

1. Dube D.H. and Bertozzi C.R., Glycans in cancer and inflammation-potential for therapeutics and diagnostics, *Nat. Rev. Drug Discov.*, **4**, 477-488 **(2005)**

2. Akinkuolie A.O., Buring J.E., Ridker P.M. and Mora S., A novel protein glycan biomarker and future cardiovascular disease events, *J. Am. Hearth Assoc.*, **3**, e001221 **(2014)**

3. Duus J.Ø., Gotfredsen C.H. and Bock K., Carbohydrate structural determination by NMR spectroscopy: modern methods and limitations, *Chem. Rev.*, **100**, 4589-4614 **(2000)**

4. Mechref Y., Kang P. and Novotny M.P., Differentiating structural isomers of sialylated glycans by matrix-assisted laser desorption/ionization time-of-light/time-of-light tandem mass spectrometry, *Rapid Commun. Mass Spectrom.*, **20**, 1381-1389 **(2006)**

5. Domon B. and Costello C.E., A systematic nomenclature for carbohydrate fragmentations in FAB-MS/MS spectra of glycoconjugates, *Glycoconjugate J.*, **5**, 397-409 **(1988)**

6. Mechref Y. and Novotny M.V., Structural characterization of oligosaccharides using MALDI-TOF/TOF tandem mass spectrometry, *Anal. Chem.*, **75**, 4895-4903 **(2003)**

7. Tan E.Z., Yin P.G., You T.T., Wang H. and Guo L., Three-dimensional design of large-scale TiO$_2$ nanorods scaffold decorated by silver nanoparticles as SERS sensor for ultrasensitive malachite green detection, *ACS Appl. Mater Interfaces*, **4**, 3432-3437 **(2012)**

8. Chang C.C., Chiu N.F., Lin D.S., Su Y.C., Liang Y.H. and Lin C.W., High-sensitivity detection of carbohydrate antigen 15-3 using a gold/zinc oxide thin film surface plasmon resonance-based biosensor, *Anal. Chem.*, **82**, 1207-1212 **(2010)**

9. Chiang C.K., Chiang N.C., Lin Z.H., Lan G.Y., Lin Y.W. and Chang H.T., Nanomaterial-based surface-assisted laser desorption/ionization mass spectrometry of peptides and proteins, *J. Am. Soc. Mass Spectrom.*, **21**, 1204-1207 **(2010)**

10. Schurenberg M., Dreisewerd K. and Hillenkamp F., Laser desorption/ionization mass spectrometry of peptides and proteins with particle suspension matrixes, *Anal. Chem.*, **71**, 221-229 **(1999)**

11. Obena R.P., Lin P.C., Lu Y.W., Li I.C., Mundo F., Arco S.R., Nuesca G.M., Lin C.C. and Chen Y.J., Iron oxide nanomatrix facilitating metal ionization in matrix-assisted laser desorption/ionization mass spectrometry, *Anal. Chem.*, **83**, 9337-9343 **(2011)**

12. Tribelsky M.I., Miroshnichenko A.E., Kivshar Y.S., Luk'yanchuk B.S. and Khokhlov A.R., Laser pulse heating of spherical metal particles, *Phys. Rev. X*, **1**, 021024-1 **(2011)**

13. Obena R.P., Tseng M.C., Primadona I., Hsiao J., Li I.C., Capangpangan R.Y., Lu H.F., Li W.S., Chao I., Lin C.C. and Chen Y.J., UV-activated multilayer nanomatrix provides one-step tunable carbohydrate structural characterization in MALDI-MS, *Chem. Sci.*, **6**, 4790-4800 **(2015)**

14. Primadona I., Lai Y.H., Capangpangan R.Y., Obena R.P., Tseng M.C., Huang M.F., Chang H.T., Li S.T., Wu C.Y., Chien W.T., Lin C.C., Wang Y.S. and Chen Y.J., Functionalized HgTe nanoparticles promote laser-induced solid phase ionization/dissociation for comprehensive glycan sequencing, *Analyst*, **141**, 6093-6103 **(2016)**

15. Koubenakis A., Frankevic V., Zhang J. and Zenobi R., Time-resolved surface temperature measurement of MALDI matrices under pulsed UV laser irradiation, *J. Phys. Chem. A*, **108**, 2405-2410 **(2004)**.